Using Seasonal Monitor Data to Assess Aviation Integrity

Sherman Lo, Stanford University, Robert Wenzel, Booz Allen Hamilton, Greg Johnson, Alion Science and Technology, Peter Swazsek, University of Rhode Island, Peter Morris, Stanford University, Per Enge, Stanford University

As we become increasing dependent on GPS for many position, navigation, and time (PNT) applications, it becomes increasing important that we have an alternate means of obtaining those capabilities. This is especially important in critical applications such as aviation. As part of the ongoing Federal Aviation Administration (FAA) Loran evaluation, the system is being assessed for its ability provide stand alone navigation capability through all phases of flight. This will allow users to retain much of the functionality enjoyed when using GPS should the system be unavailable.

For Loran to be used for aviation navigation, it must meet the integrity requirements of that application. A key requisite for meeting integrity is the ability to bound position errors to a high degree of confidence. This, in turn, means bounding range domain errors and variations. One major source of variation is the temporal variation of propagation delay known as additional secondary factor or ASF. Models were developed to provide the bound on the ASF variations for the assessment of Loran aviation coverage. These bounds are designed to meet the integrity requirements on the error. Significant amounts of high quality Loran data from the U. S. Coast Guard (USCG) has been used to generate the model. This, however, left little data of adequate quality to perform the independent assessment of the models' performance. Hence, little or no independent validation of the efficacy of the bounds could be done until recently.

This paper presents preliminary analysis of the validity of the models for bounding the temporal variation of ASF. It uses data collected in 2006 from seasonal monitors set up by the FAA Loran evaluation team. It will examine both the performance of the bounds in the range and position domain. Selected sensitivity will be examined to test robustness of the model and implementation.

1.0 Introduction

Additional secondary factor (ASF) is the extra delay on the time of arrival (TOA) of the Loran signal due to propagation over nonhomogenous land path vice an all seawater path. This delay can be significant and will result in position errors of hundreds of kilometers or more should it not be accounted for. As such, reasonable estimates of ASF are necessary for accurate positioning using Loran. The result is that most modern receivers utilize a static estimate of ASF. However, even with good ASF estimates, significant position errors may result as the ASF varies temporally. The temporal variation of ASF can be on the order of half a kilometer over the course of a year. This represents the largest source of error on Loran. If not properly accounted for, it can pose a problem when Loran is used for safety of life applications, such as aircraft navigation and landing.

One goal of enhanced Loran (*eLoran*) is to support aircraft navigation and landing. Specifically, it means that *eLoran* will have to meet the requirements of non precision approach (NPA) operations such as LNAV, which permits a 350 ft decision height [1]. Meeting the integrity requirements means that the position errors are bounded to a high confidence level. This means each error source must be adequately bounded. As the temporal variation of ASF is the largest such error source, it is critical to bound this error. However, the bound cannot be too excessive as it would make the system unavailable for the desired operation.

As such, the Federal Aviation Administration (FAA) Loran Technical Evaluation team developed models for bounding the temporal variation of ASF. This paper will detail the analysis of data to validate the model and to examine the conservatism of the model. The first section of the paper will discuss background on the temporal ASF variation bound methodology and models. The next section will describe the source and collection of the data used for the assessment. The body of the paper will compare the collected ASF and its resultant model bound. It will examine this in the range domain and project that comparison to the position domain. The final part of the paper will assess the sensitivity of the model to specific errors.

2.0 Background

The section describes the methodology used to bound the temporal ASF variations. The methodology requires two components – an estimate of the seasonal midpoint value of ASF and a model that bounds the peak to peak temporal ASF variation. The seasonal midpoint represents the nominal ASF that the user receiver applies. It is about this nominal value that the bound is applicable. These two parts are illustrated in Figure 1. The Loran evaluation team is still working on its preferred methodology for determining the seasonal midpoint and this portion will not be discussed. The models developed to bound the peak to peak temporal ASF variation will be described later in this section.

2.1 Bounding Temporal ASF Variations

In order to conduct an evaluation of Loran for NPA, it was necessary to develop a model for the temporal variation of ASF. The assumption is that the receiver would store and apply some nominal value (or values) of ASF. Application of this nominal value results in a residual or corrected ASF (*ASFc*). The temporal ASF bound ($ASFbound_{temp}$) would bound the maximum excursion from this value which is just the maximum absolute value of *ASFc*. Using the seasonal midpoint ASF ($ASF_{temp,midpt}$), as defined by Equation 1, results in the smallest possible temporal ASF bound. The basic premise is seen Figure 1. Thus, it is quite reasonable to expect the inequality expressed in Equation 2 to hold if we wish to have an adequate position domain bound. However, this is not a necessary condition for a variety of reasons. The bound though serves as a good first order check that we are on the right track.

When considering the worst case, initial analysis suggests little advantage in terms of integrity for the receiver to use multiple nominal values of ASF during the year [2]. This is because winter variations can span much of the entire range. Hence bounding the winter essentially requires bounding the entire year range. As result, we used a bound that is suitable for the entire year. Since the bound requires a nominal value about which it applies, we chose the midpoint value of ASF. The choice was selected since it minimizes the maximum excursion resulting in the smallest overall bound.

Define $ASF(t) = ASFc(t) + ASF_{temp,midpt}$ & $ASF_{temp}^{peak-peak} = \max\left(ASF(t)\right) - \min\left(ASF(t)\right)$

$$ASF_{temp,midpt} = \frac{1}{2}\left(\max\left(ASF(t)\right) + \min\left(ASF(t)\right)\right) \quad (1)$$

$$\max\left|ASFc(t)\right| = \tfrac{1}{2} ASF_{temp}^{peak-peak} \le ASFbound_{temp} \quad (2)$$

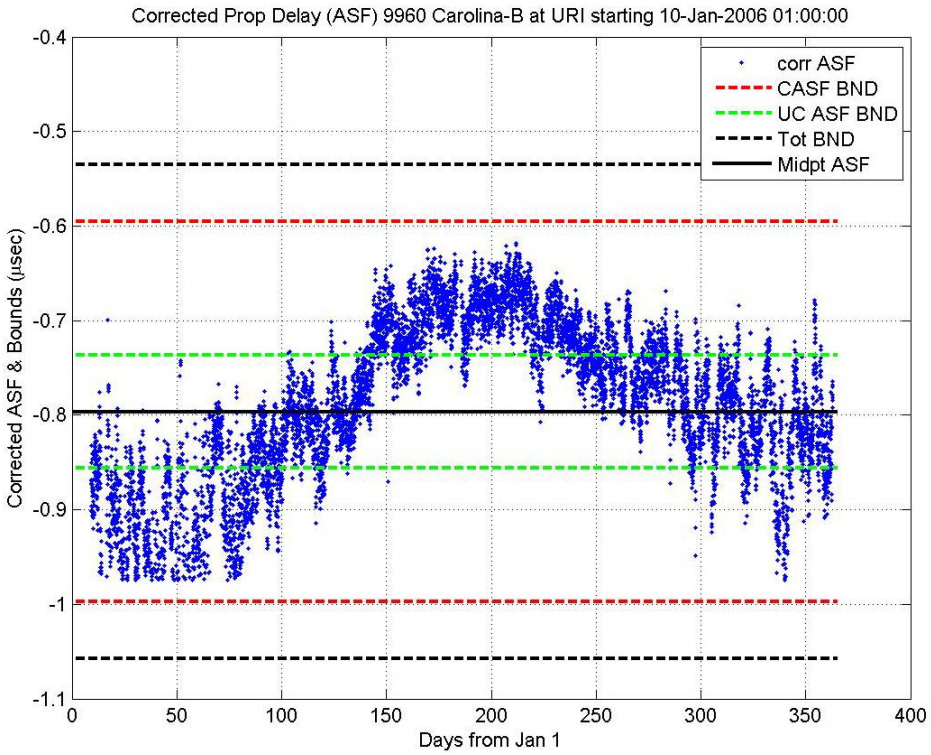

Figure 1. Example showing Correlated, Uncorrelated bounds on temporal ASF variation and estimated Midpoint ASF

2.2 Discussion on ASF Components

Different forms of error are affected differently by the position solution. For example, error or variations common to all measurements essentially do not affect the position solution. The cumulative effect of common mode errors, meaning errors that are the same on all signals, is calculated by the traditional navigation least squared solution used by Loran and GNSS along with the position. It is only the residual variations after

removing the common terms that affect the position solution. In addition to common error, the variation can be further divided into different categories. We can create bounds for each category so that the overall combination will bound in the position domain. In our model, the bound variation is separated into two components: correlated and uncorrelated.

2.3 Models for Peak to Peak Temporal ASF Variations

It is very important that the temporal ASF into is divided into correlated and uncorrelated components. The correlated ASF is the portion of the temporal ASF seasonal variation is related to path length. As such, it can be considered to move in a similar direction for all received signals. The uncorrelated temporal ASF is the residual error. It is the portion of the temporal ASF that cannot be considered to move in a similar direction as all other signals. Therefore, this portion must be treated in the worst case combination. The division allows for some of the ASF bound variation to be treated in a related manner rather than in the worst case combination. Physics suggest that the division is realistic as some of the ASF variation between different signals is correlated as they share some common weather and land regions. The properties of the propagation region determine the ASF. This separation into these two components also has historical precedent dating to work by Johler and Doherty [3][4].

The division is of significant importance when it comes to developing a position domain bound that is not overly conservative. This is because, when generating the bound on horizontal position error (HPE), known as the horizontal protection level (HPL), the correlated ASF bound can be combined directly while uncorrelated must be combined in a worst case manner. Two basic models were developed and their development is described in [2]. This is discussed in the next session.

A conservative bound in the range domain would have both the correlated and uncorrelated components bounded. Bounding would seem to require that Equation (3) holds. However, that is not completely the case. Furthermore, there are some caveats. The most important is that the uncorrelated component must be bounded due to the worst case treatment. Its contribution to the HPE bound is much greater than that of the correlated. That is, one meter of uncorrelated bound results in a much larger bound in the position domain than does one meter of correlated bound. As such, the uncorrelated ASF bound can be used to bound any correlated ASF variation that is not covered the correlated ASF bound. Hence, it is not an integrity issue we underestimate the correlated component provided that there is an additional amount uncorrelated bound that covers the underestimated portion. Another way of thinking about this is that the correlated variations can be underbounded provided that the uncorrelated bound "covers" the underbound.

$$\left|ASF_{temp}(t) - ASF_{temp,midpt}\right| = \tfrac{1}{2} ASF_{temp}^{peak-peak} \le \left(ASFbound_{temp,corr} + ASFbound_{temp,uncorr} + common\right) \quad (3)$$

2.3.1 Models for 2004 Report

For the 2004 FAA technical evaluation, a bound model was developed to determine Loran NPA LNAV coverage. Past Loran data and studies were used as the basis of the model. Specifically, the West Coast (1985), NEUS/SEUS signal stability report (1983). As there was no mid-continent data in the 1980s (and hence it was not studied), 2002-2003 Loran Operations Information System (LOIS) data was analyzed to provide values for the mid-continent. The goal of these historical (1980s) studies was not to determine a bound but rather to determine the best ASF to use and statistics on the variation of ASF. Accordingly, some analysis and reinterpretations of those results were necessary. This model (termed 2004 intended model) was incorporated into the Loran aviation coverage tool [5]. In the translation, the calculation of the uncorrelated term changed, resulting in a slightly less conservative bound. This model was used in the 2004 report and will be termed the 2004 report model or Model 1 for the purpose of discussion. Additionally, we will refer to the 2004 intended (revised) model as Model 2.

2.3.2 Weather Regression Model

After the 2004 report, it was felt that the 2004 model lacked the desired resolution and preciseness. Additionally, it was hoped that some of the conservatism of the model could be reduced. And so, a model based on high density weather data was developed. The model is based on the dry component of index of refraction (N_{dry}), a term that is known to be correlated with changes in Loran propagation speed. A map for generating the temporal ASF bound was developed based on weather measurements from over 1400 National Oceanic Atmospheric Administration (NOAA) sites. For this paper, we term this model the weather regression model or Model 3.

2.4 Calculating Model Bounds from Map

Essentially, the models are used in a similar manner and outputs the correlated and uncorrelated bounds for the temporal ASF variation. However, the underlying maps of for weighting the effect of propagation path are different between baseline models. The calculation starts by taking an integral over the path between the user and the transmitter used. This integral is weighted by the underlying map values. Denote the value of the integral as *d*. This value is then used to derive the correlated and uncorrelated component. The underlying map for the 2004 model and the weather regression model are different and hence the integral will result in different values.

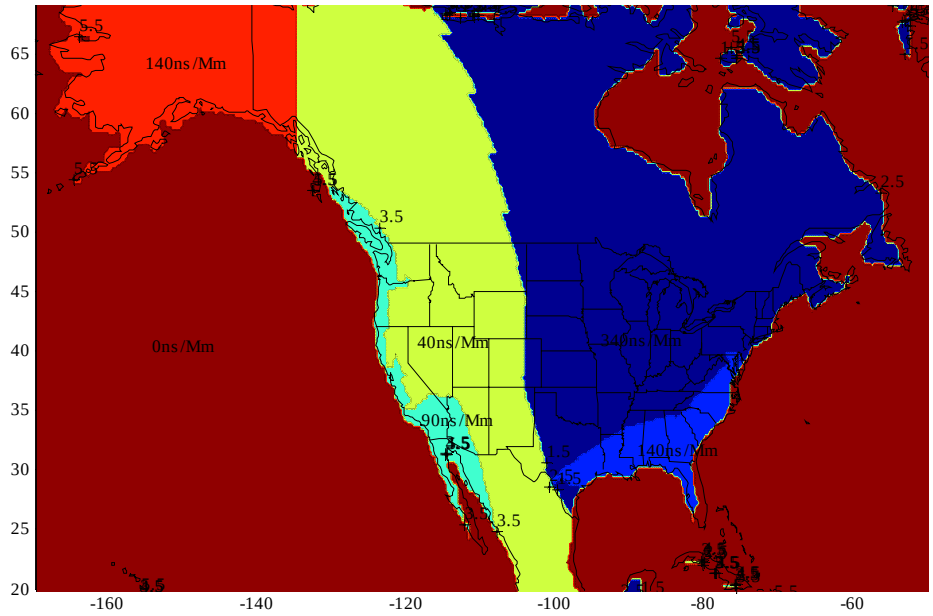

Figure 2. Map of Different Regions Affecting Temporal ASF Variations for 2004 Models

The map for the 2004 models relating the relative propagation path effects on temporal ASF variation is seen in Figure 2. The values shown on the map are related to the correlated component. While the values may be different, the correlated and uncorrelated models utilize the same regional divisions. Determination of the correlated portion is calculated by taking the path integral over the map using the values in each region. The result is a root mean squared (rms) value of the temporal variation/deviation. Hence, we multiplied by a factor of 2.95 to transform the rms value to an absolute bound. The 2.95 was derived empirically. Determination of the uncorrelated component uses the same map though the values for the regions are different. This is seen in Table 1. As mentioned, the 2004 report model was revised. The only difference between the report and revised model is with the calculation of the uncorrelated component. The uncorrelated component was meant to be fixed term regardless of path length. If the path traverses several regions, the uncorrelated component is the fixed component of the regions weighted by percentage of path in those regions. Mathematically, it is calculated as the sum of the fixed value for those regions multiplied percentage of the path in those regions.

The calculation of the correlated and uncorrelated components of ASF variation using the weather regression model is reasonably straight forward. Using the map seen in Figure 3, the correlated and uncorrelated components are calculated using Equations (4) and (5), respectively. Table 2 provides a summary on the calculation of the ASF bounds for each model.

Region	Corr (σ_{dTD})(ns/Mm)	Uncorr (report) (ns/Mm)	Uncorr (revised) (ns)
1	0	0	0
2	40	200	200
3	90	100	100
4	140	150	150
5	340	250	250

Table 1. Regional Weights for Correlated and Uncorrelated Temporal ASF for Model 1 & 2

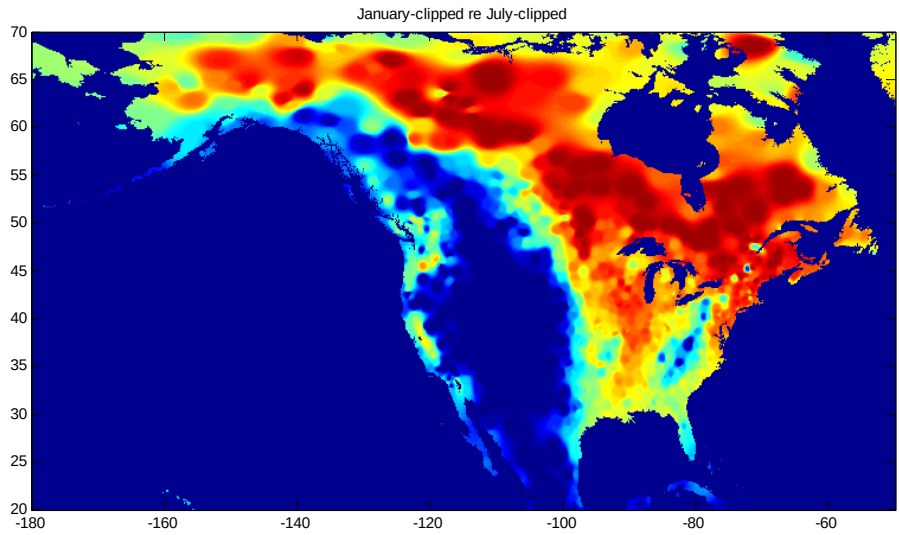

Figure 3. Map of Different Regions Affecting Temporal ASF Variations for Weather Model

Correlated ASF bound = 3.0636*d μsec = 0.9184*d m (4)

$$ASF_{uncorr,\max} = 1.32\sqrt{\frac{d+16.36}{1636.905}}\mu\sec \quad (5)$$

	Report 2004 (Model 1)	**Intended 2004 (Model 2)**	**Weather Regression (Model 3)**
Correlated Bound (μsec)	2.95*d/1000 μsec	2.95*d/1000 μsec	3.0636*d μsec
	0.8824*d m	0.8824*d m	918.4*d m
Uncorrelated Bound (μsec)	d*/1000 μsec where d* is path integral using uncorrelated weights	d'/1000 μsec where d' is path percentage weighted value of uncorrelated bias	$1.32\sqrt{\frac{d+16.36}{1636.905}}\mu\sec$
	0.29979*d*	0.29979*d'	$395.7\sqrt{\frac{d+16.36}{1636.905}}m$

Table 2. Calculation of Correlated & Uncorrelated Temporal ASF Variation (3 Models)

2.5 Data for Assessment

While the US Coast Guard (USCG) has gathered significant data on Loran over the past years, there is a need for additional data for validation. Part of the reason is due to the fact that the USCG data was used to develop the models. For example, data from USCG LRS IIID taken between May 2003 to September 2004 was used to develop relationship between N_{dry} and ASF (Time Interval Number (TINO) data taken from Remote Automated Integrated Loran (RAIL)). Additionally, there is a need for a data source from which we can directly measure ASF with minimal contamination from other sources of TOA variations.

As part of the FAA evaluation, seasonal Loran monitors were set up throughout the Northeast United States. The monitors are currently located in Boston (Volpe National Transportation Center), MA, University of Rhode Island (URI), RI, US Coast Guard Academy (USCGA), New London, CT, Ohio University, Athens, OH, and Atlantic City, NJ. Additional monitors will be installed in 2007. These seasonal monitors provide data to support the evaluation including the assessments of differential Loran and ASF. The seasonal monitor set up is seen in Figure 4. It is composed of four major components: data collection computer, GPS steered rubidium clock, a universal counter and a Locus Satmate or LRS IIID Loran receiver. The Locus receiver provides the processing of the data. The Locus provides one minute output of various parameters such as time of arrival (exponential average), signal to noise ratio (SNR), envelope to cycle difference (ECD), etc. The system reset itself at midnight UTC (Universal Time Coordinated) to prevent clock errors from persisting over long (days) periods of time.

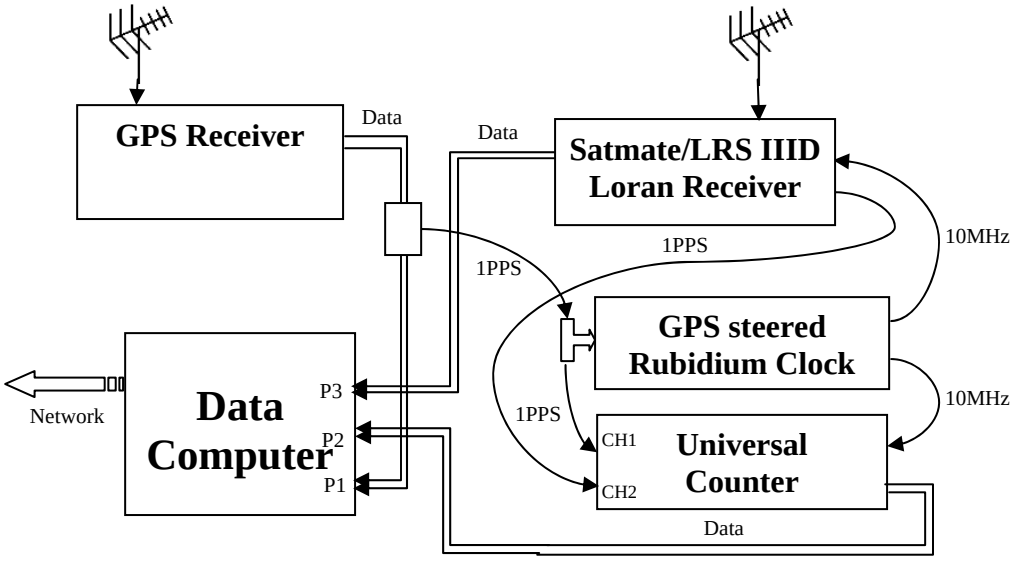

Figure 4. Set up of the Seasonal Monitors

The raw data has outliers and other discontinuities and variations not related to ASF due to installation, processing or other factors. The data was processed to remove as many of these points as possible without removing actual ASF phenomena. This is discussed later.

2.6 Calculating HPL Bounds

The Loran integrity or HPL equation is given in Equation (6). This equation governs the bounding of the horizontal position error of which the contribution of the temporal variation of ASF is only a component. Of concern to the bounding of the temporal variation are the second and third terms of the equation which deal with how to add correlated and uncorrelated biases.

$$HPL = \kappa \sqrt{\sum_i K_i \alpha_i^2} + \left| \sum_i K_i \beta_i \right| + \sum_i \left| K_i \gamma_i \right| + PB \qquad (6)$$

The second term of the equation relates to completely correlated biases. This is used to bound the temporal variation in ASF that is correlated with our weighted land path integral discussed in Section 2.2. Since these errors are correlated, the confidence bounds for these errors can be added together before taking the absolute maximum. In other words, because of the correlation, we do not have to take the worst-case combination. When examining the temporal variations, β represents the absolute bound on the correlated component.

The third term accounts for bias errors that are uncorrelated. The confidence bounds, γ, for these errors can be added together in the worst-case combination. For the temporal variations, γ represents the absolute bound on the correlated component.

The matrix K comes from the weighted least-squares pseudoinverse matrix that determines the position solution. It is derived from the geometry matrix G which relates pseudorange measurements (y) to the position solution (x) and the weighting matrix, W, used to weigh the relative confidence of each pseudorange measurement. This seen in Equations (7) and (8).

$$\hat{x} = (G^T W G)^{-1} G^T W y \equiv K y \qquad (7)$$

$$y = Gx + \varepsilon \qquad (8)$$

Hence the contribution of the temporal variation of ASF to the HPL is given by Equation (9). In Equation (9), β_i and γ_i represent the absolute bound on the correlated and uncorrelated component of the temporal variation of ASF for station i.

$$HPL_{tempASF} = \left| \sum_i K_i \beta_i \right| + \sum_i \left| K_i \gamma_i \right| \qquad (9)$$

3.0 Assessing the Model Bound

In order to assess the model bounds, we had to go through three steps:

1) Calculate the correlated and uncorrelated ASF bound for each station used
2) Calculate the resulting position domain bound (viz, the component of HPL that bounds the temporal variation of ASF)
3) Calculate the error the seasonal monitor due to the temporal variation in ASF

Section 2 discussed the models used for step achieving steps 1 and 2. Step 3 is admittedly difficult as our measurements also contain noise, interference, and other errors. Some of the obvious errors were removed in the filtering process. Additionally, averaging reduces random error such as noise. Indeed, the averaging used is far in excess of what is possible in aviation. However, the additional errors should be generally small. In fact, its presence should only increase the conservatism of the analysis.

3.1 Past Assessment of 2004 Model with LRS IIID

Our first large scale assessment of the 2004 model utilized USCG TINO data from May 2003 to September 2004 taken using from monitor receivers (Locus LRS IIID). While this data was later used to derive the weather regression model, it represents an independent data source for validating the 2004 model. These cases are somewhat discussed in [2].

Generally, the errors were bounded in the position domain. In 82% (64) cases, the position domain bound was more than 24% larger than the maximum errors. There were 4 cases where maximum error was within 20% of the position domain bound. However, there were ten problem cases where due to the position error was underbound. In two of the cases, which are seen in Figure 5, one point caused the underbounding. This led us to believe that it was due to an outlier from the Grangeville signal. However, initial examination does not provide clear confirmation of that hypothesis.

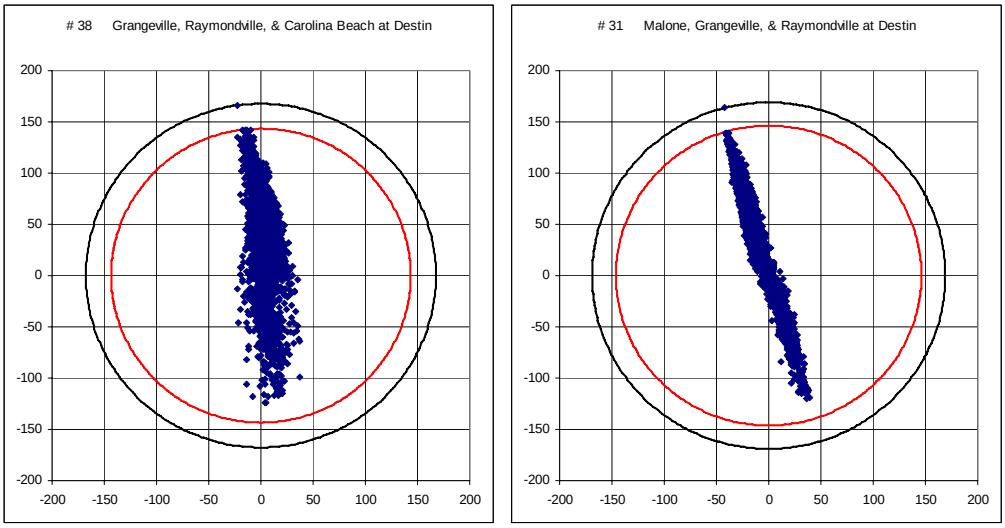

Figure 5. Comparison of the Position Error (max in black circle) vs. position bound (red circle)

In the other cases, the difference between the bound and maximum error were due to multiple points. In the worst case the maximum error exceeded the bound by up to roughly 20%. If the correct uncorrelated ASF values were used (Model 2 instead of Model 1), it is expected that the maximum errors would have been bounded. These results provide confidence in the model but also pointed out issues that need to be resolved.

3.2 2006 Seasonal Monitor Data

The establishment of the seasonal Loran monitors for the assessment of *eLoran* provided us with another independent source of data for validating the bounds. The data cannot be used directly as there are cycle slips, timing glitches and other outliers. Additionally, there is random noise on the measurement which cannot be removed. At a minimum, the data must be examined to remove obvious outliers and other artifacts that are not reflective of ASF.

Some basic processing was used to remove outliers. First obvious jumps and glitches were removed. Afterwards, since it is unlikely that ASF will have large discontinuous jumps, a running average filter was used to remove such outliers. The processing is presented in Table 3. While some non ASF related errors still remain, these basic filters allow us to focus on predominately ASF effects. The desire is to retain all ASF effects, no matter how extreme. This is essential as we care about the worst case deviation caused by ASF. Figure 6 and Figure 7 show an example of the data prior to and after filtering, respectively.

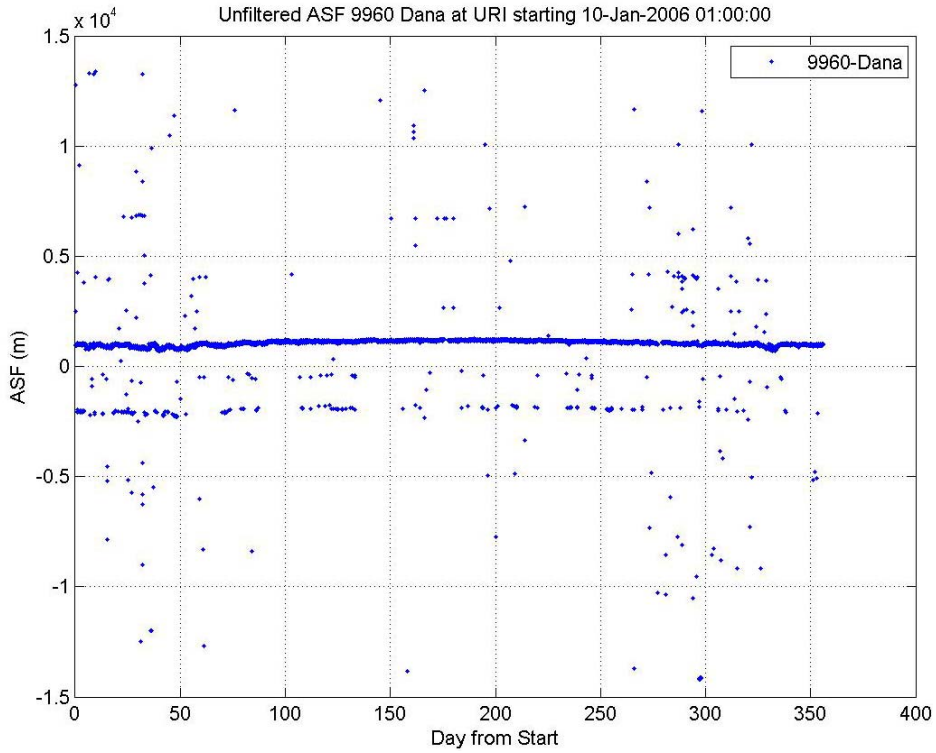

Figure 6. Unfiltered Estimated ASF from Dana as measured at URI (2006)

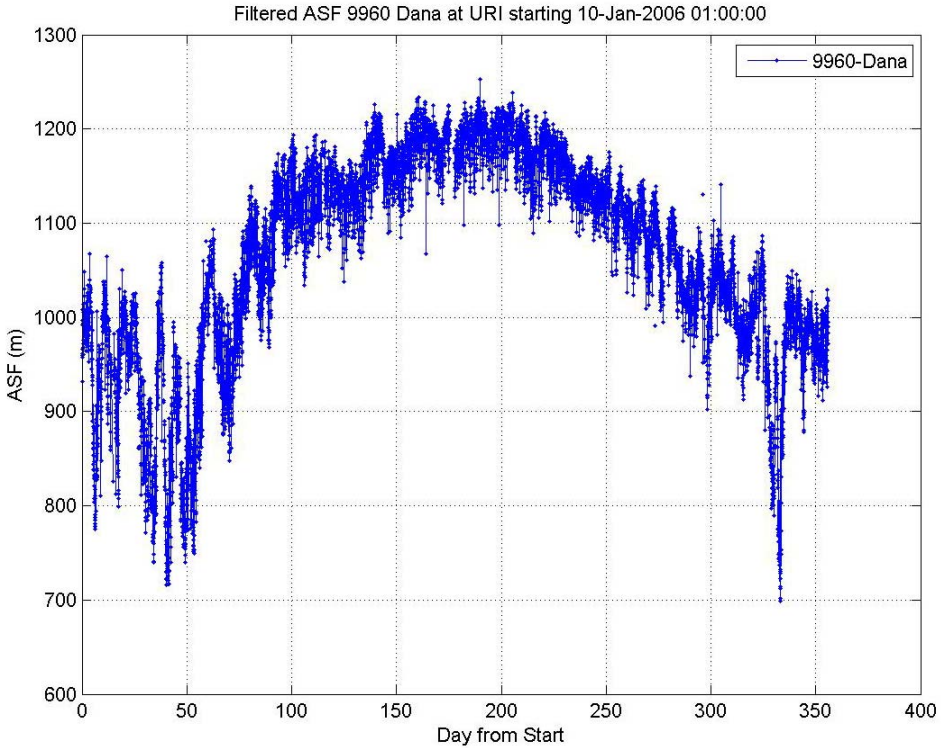

Figure 7. Filtered Estimated ASF from Dana as measured at URI (2006)

Filter	Design	Objective
1	Eliminate points > 0.6 cycle away from median value	Eliminate cycle slips and large outliers
2	Eliminate points larger than 1 standard deviation from a running average	Eliminate large discontinuous jumps

Table 3. Basic Filtering of Data to Eliminate Outliers

As a note of interest, we will discuss some of the data outlier issues discovered. Some issues were due to system set up. One thing that was noticed was timing errors that coincided with the beginning of the UTC day. This was due to the data collection set up which reinitialized the time at midnight UTC. Since it took time for clock to settle down, the first couple of data points were invariably skewed by timing errors. The solution to this problem was to throw out the first couple of data points. Other issues were related to the site location. For example, it was noticed that USCGA seemed unusually noisy through out the summer. When inspected, it was discovered that the antenna was sited at a location close to air conditioning system that resulted in the increase noise in the measurements.

3.3 ASF Variation vs. Model Bound

After filtering the data, we can compare the ASF variation to the bounds derived by the models. First, we begin be calculating the midpoint ASF value for each station used. That point is set to be our nominal zero ASF error value. Centering the data, we can compare the result to the correlated, uncorrelated and total temporal ASF bound. An example of this for the Seneca signal as seen at Volpe using the Weather Regression Model is seen in Figure 8. As seen in the figure, some outliers remain (e.g. circa day 270). This is because the goal of the filtering is to remove obvious outliers while retaining the maximum true variation. If the filtering is too aggressive, some of the true variation may be lost.

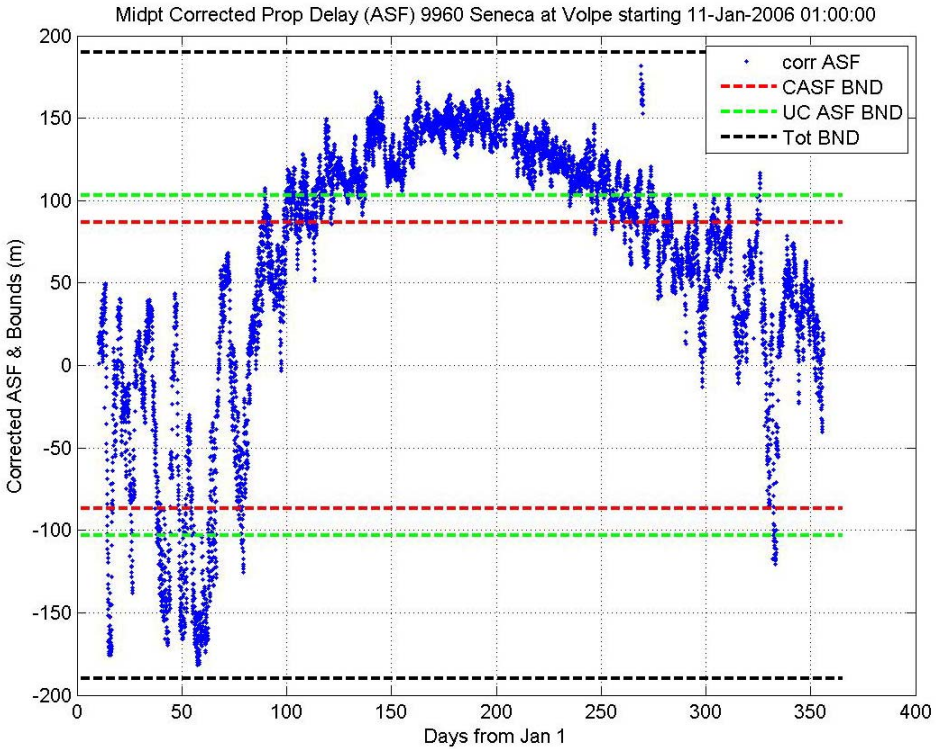

Figure 8. Estimated ASF from Seneca & Bound (Weather Model) as measured at Volpe, MA

In most cases examined, the total bound does overbound the variations. Figure 9 and Figure 10 show the results for the Seneca, NY and Caribou, ME signals, respectively, as measured by four seasonal monitor stations. The charts compare the correlated and uncorrelated errors to the maximum error (deviation from the midpoint) over the course of the year.

There are some cases in which the models do not overbound the maximum error. Usually, this occurs for nearby transmitters. One issue may be that common error terms are not removed. Two other likely contributors are measurement noise and map coarseness. These two sources, particularly when the location is near the transmitter, can conspire to result in underbounding.

When close to the transmitter, measurement noise generally contributes a greater fraction of the total measurement error than when further away. Hence, the ASF variation is less more visible when near the transmitter. This is due to the fact that the dominant measurement noise is due to transmitter jitter which is not path length dependent. As we move further away, the overall measurement noise increases a bit due to signal attenuation but not at the same rate that ASF increases. Eventually, this reverses since signal attenuation due to path loss becomes dominant. We will need to investigate these cases in more detail to determine whether the models are adequate. Necessary testing includes zero baseline measurements to determine noise levels.

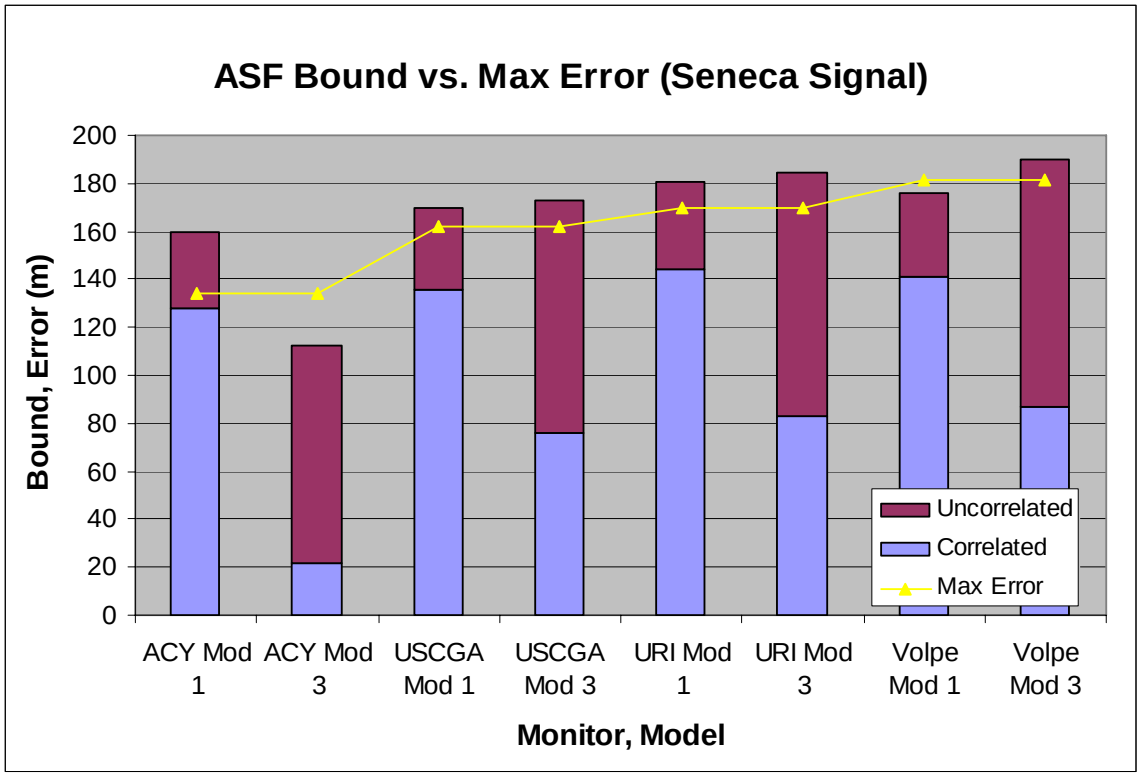

Figure 9. Temporal ASF Bound vs. Max Error for the Seneca, NY Signal at 4 Monitor Sites (2006)

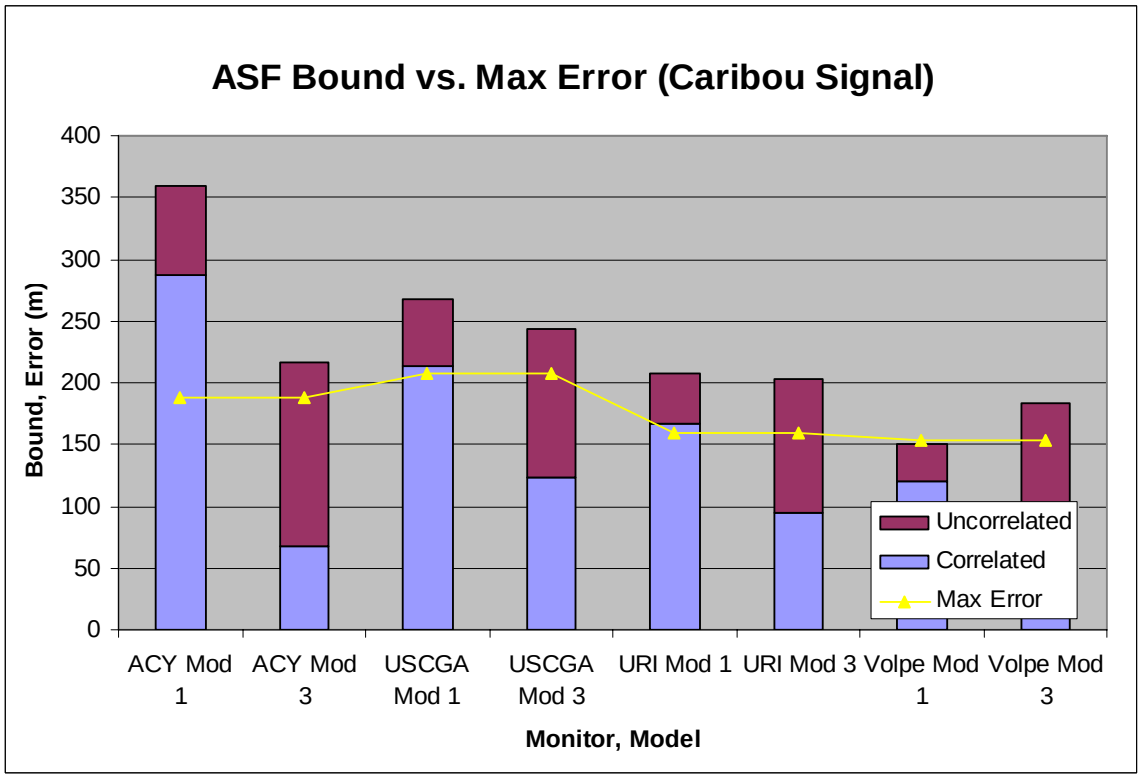

Figure 10. Temporal ASF Bound vs. Max Error for the Caribou, ME Signal at 4 Monitor Sites (2006)

Map coarseness is another cause of underbounding. The effect can be seen in the following example. Figure 12 shows the results for Nantucket at Volpe with bounds generated by the 2004 model. Due to the coarseness of the map, the model assumes an all seawater path when this is clearly not the case (as seen in Figure 11). In fact, almost all of the Nantucket measurements for both models are not adequately bounded. This is seen in Figure 13. It is suspected that the model map coarseness and noise on the measurement combine to produce the result. Some confirmation is provided by examining the results of the weather regression model. The bounds for the weather regression model are far larger than and much closer to the maximum error when compared to the 2004 model. This is because the 2004 model has a much coarser map than the weather regression model, as seen previously.

As we move farther away, the bound generally covers the maximum error. This can be seen in the Nantucket data as well where Model 3 does bound the maximum error at the Atlantic City. Atlantic City is much farther away from Nantucket than the other three monitors.

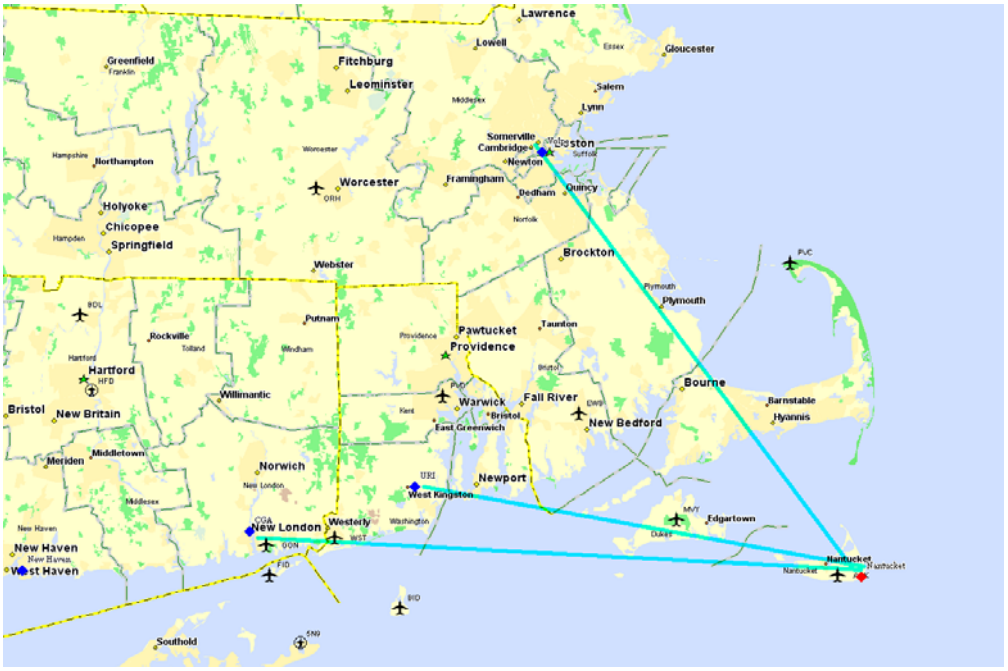

Figure 11. Propagation paths for the Nantucket Signal to USCGA, URI, and Volpe (West to East)

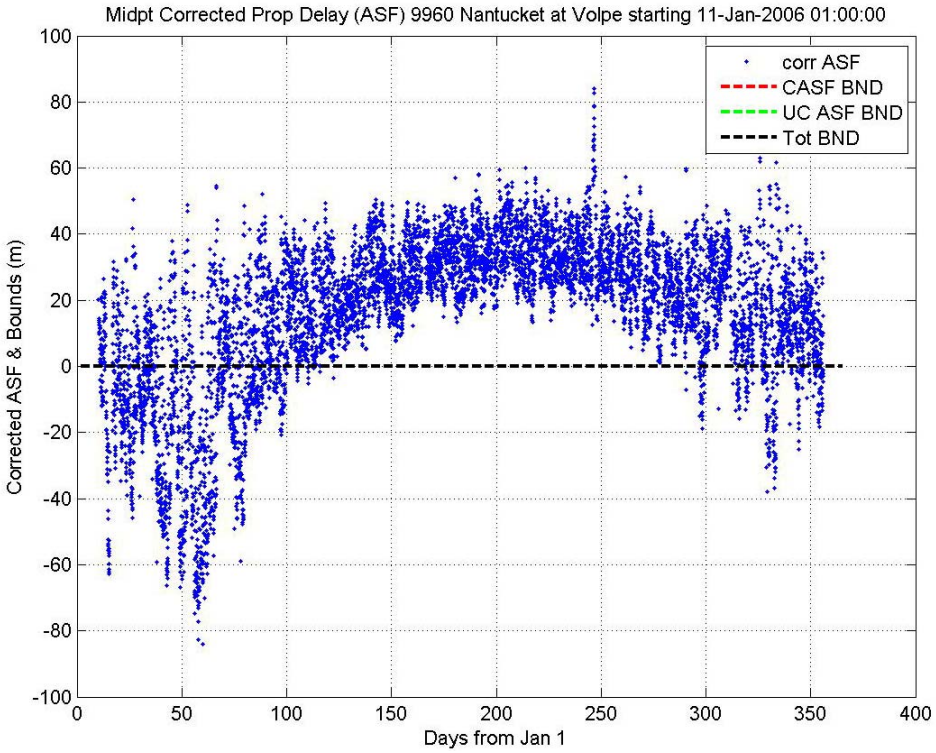

Figure 12. Estimated ASF from Nantucket & Bound (2004 Report Model) as measured at Volpe, MA

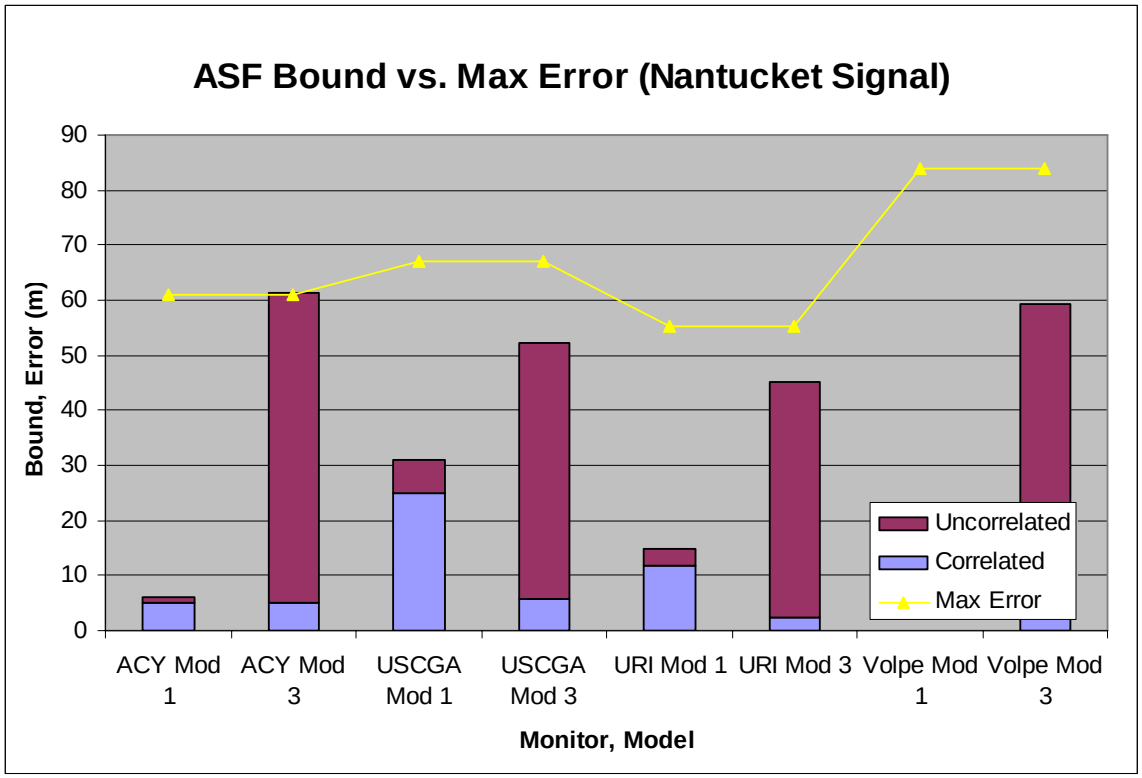

Figure 13. Temporal ASF Bound vs. Max Error for the Nantucket, ME Signal at 4 Monitor Sites (2006)

Having the total bound overbound the variations is not a necessary condition. The more important condition is that the uncorrelated bound be larger than the true uncorrelated variation. This is because the uncorrelated biases are treated more conservatively than the correlated in the integrity equation. We will see that the total bound for the Weather Regression model is generally lower than that for the 2004 Report model. However, in the position domain, the weather regression model has a significantly larger bound. This is because it generally has a larger value of uncorrelated bound than the 2004 model. Future analysis will assess the breakdown of the ASF measurements into its correlated and uncorrelated components.

3.4 Position Error vs. HPL Bound

Now we can calculate the position error due to temporal ASF and compare that with its associated HPL. This is calculated using Equation (10). Error is calculated if ε is the selected to be deviation of ASF from the midpoint (*ASFc*) value for all stations. One implicit assumption from this step is that the midpoint ASF values used for each station measurement represents the zero position error value. This assumption may in fact be incorrect and will be examined in the next section. The result is the position domain error vector, *E*. The vector *E* gives our errors in the horizontal plane as well as the clock error. Figure 14 and Figure 15 show the result of the calculation over the course of 2006 for Volpe using the 2004 Report Model. The HPL is calculated using Equation (9) applied to the ASF bound components.

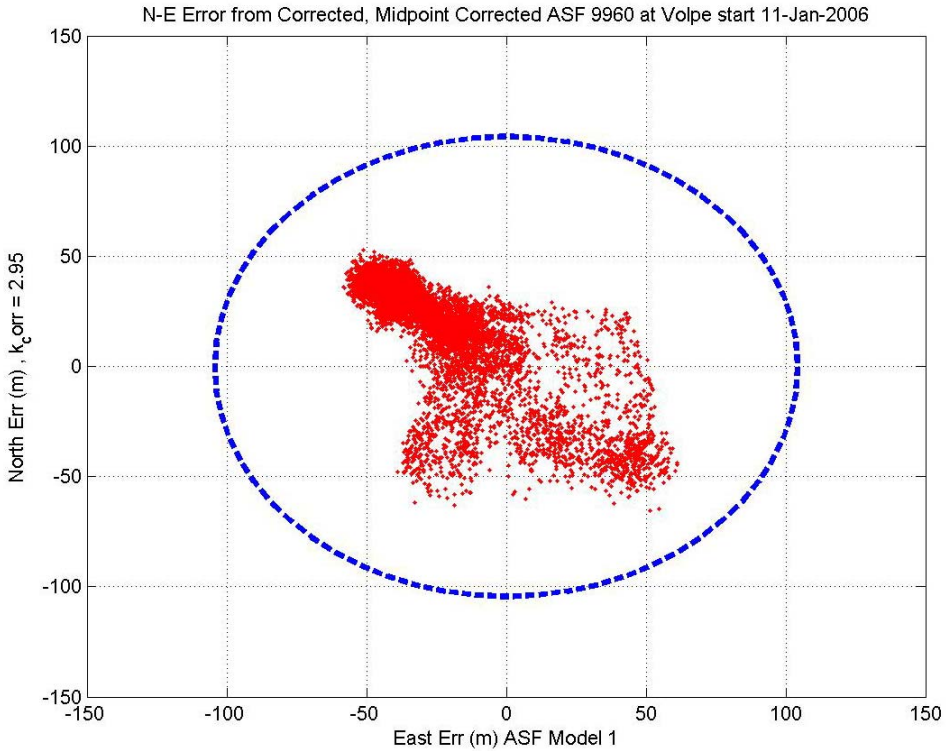

Figure 14. Scatter Plot of Position Errors and HPL from Temporal ASF at Volpe, MA using 2004 Report Model

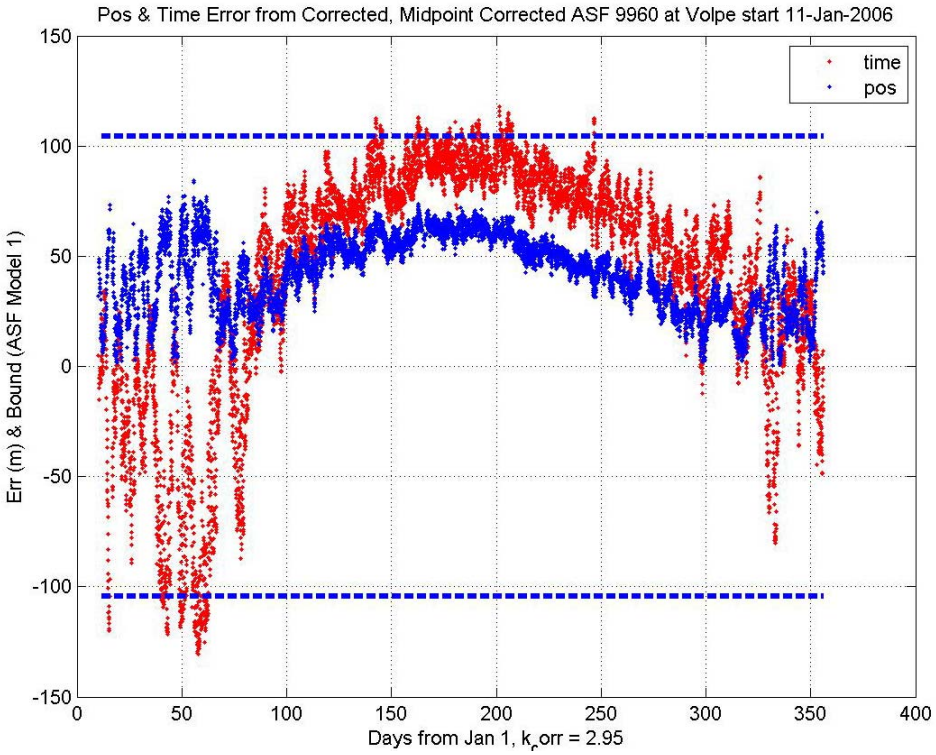

Figure 15. Time Plot of Position and Time Error along with HPL Bound from Temporal ASF at Volpe, MA using 2004 Report Model

$$E = K\varepsilon \qquad (10)$$

3.5 Summary and Observations

Table 4 shows a summary of the position bound generated for each model at each seasonal monitor site. Compared to those bounds is the maximum nominal (no error in midpoint estimation) error. As seen, the model bounds easily bound the maximum error with the weather regression model being more conservative in all cases. This is despite the fact that with the exception of close stations like Nantucket or measurements affected by map coarseness, the 2004 Report model bounds are generally larger than those of weather regression model. This can be seen in Figure 16 which compares the bounds at Ohio. In this case, the 2004 report model is larger than the weather regression model for all total ASF bounds. However, as seen in the table, the position domain bound at Ohio from the weather model is about 45% larger than the 2004 model. The result is due to the fact that the weather model has larger uncorrelated bias bounds. This emphasizes the importance of the uncorrelated bound as dominating the bound in the position domain.

Location	Volpe	URI	USCGA	Atlantic City	Ohio U
2004 Model (HPL)	104.1747	151.7882	180.0869	122.5328	132.3718
Weather Model (HPL)	148.4193	195.0466	222.1352	137.887	191.4638
Max Err (Nom)	84.4826	100.9524	141.9671	82.6268	100.2864

Table 4. Summary of HPL from Temporal ASF & Maximum Error at Monitor Sites (2006)

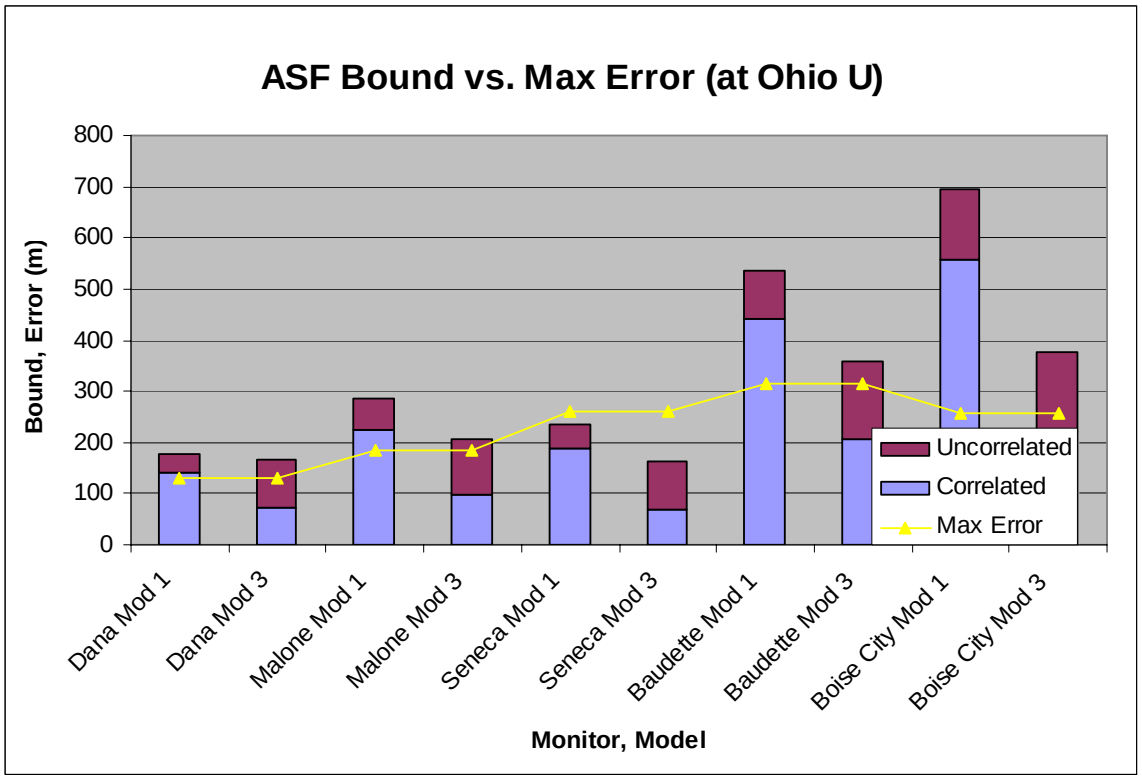

Figure 16. Comparison of Max. Error, 2004 Report & Weather Regression Model Bounds at OU

4.0 Sensitivity of Results - Assessing Errors in estimating Seasonal Midpoint

The model bounds assumed that the seasonal midpoint value of ASF is known and accurate. However, it is likely that our determination of the seasonal midpoint will have some errors. These errors can be incorporated by inflating the uncorrelated ASF bound by the appropriate level of uncertainty. However, this is likely to have a deleterious effect on availability especially if the uncertainty is too great. Since there is some conservatism inherently built into the model, some of the uncertainty may be accommodated. The question is "how much uncertainty in the seasonal midpoint ASF is acceptable (HPL bounds position domain error for temporal ASF)?"

We can answer this question by examining the position bound performance in the presence of an error in midpoint estimate. The seasonal monitor data can be used to get a first cut at how large the uncertainty can be while still bounding the position domain error. Error in the seasonal midpoint estimate was introduced to see its effects. The error in the estimate was taken as a percentage of the overall peak to peak value. Additionally, the worst combination of the error was selected. This means that relative sign on the error for each station was chosen so that the overall combination would result in the largest possible position error. Our analysis showed that a 10% error was acceptable in for all

the monitor sites examined. Figure 17 shows an example result for Volpe with a 10% error on each midpoint estimate chosen to add in the worst case manner. Table 5 shows the comparison of the bound to the maximum error for the nominal case and the case with 10% error in the midpoint estimate.

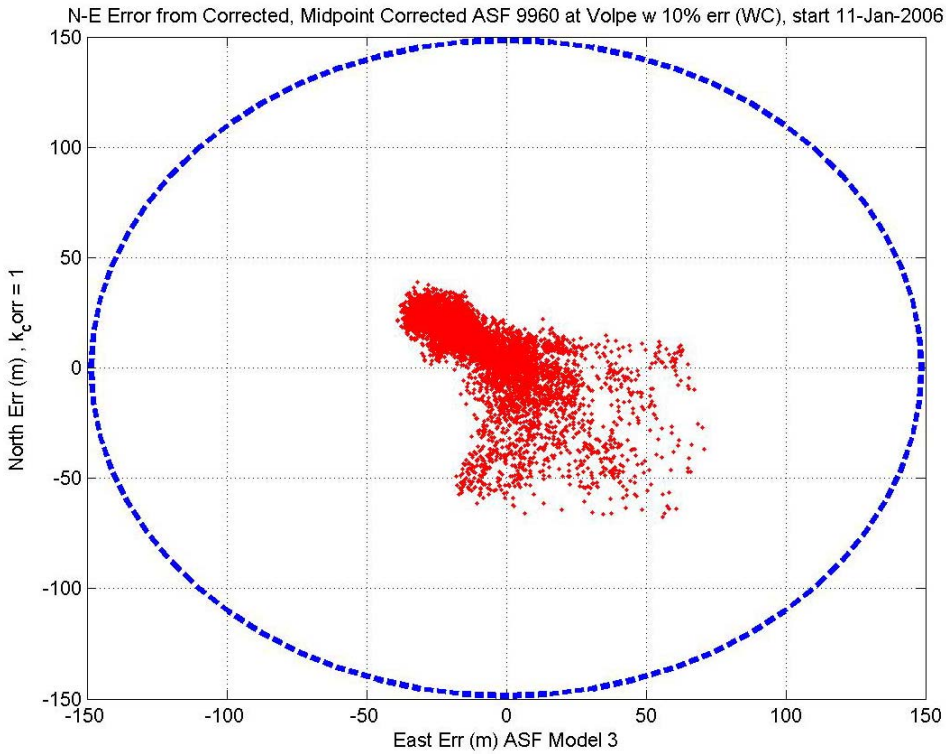

Figure 17. Position Domain Error for Volpe in 2006 with 10% error in midpoint ASF estimate chosen to add in the worst manner

Location	Volpe	URI	USCGA	Atlantic City	Ohio U
Model 1 (HPL)	104.1747	151.7882	180.0869	122.5328	132.3718
Model 3 (HPL)	148.4193	195.0466	222.1352	137.887	191.4638
Max Err (Nom)	84.4826	100.9524	141.9671	82.6268	100.2864
Max Err (10%)	100.007	118.9679	166.195	97.6874	129.7506

Table 5. Comparison of HPL from Temporal ASF & Max Error with Worst 10% Midpoint ASF Rstimation Error at Monitor Sites (2006)

5.0 Conclusions

Integrity models for any aviation navigation system need to be developed and validated. The Loran integrity performance panel (LORIPP), the multi organizational team charged with assessing Loran for aviation, has developed models for bounding much of the errors and variations experienced by the Loran user. One of the largest is the temporal variation of ASF. The models used for this have been developed using physical principals and

analysis of data. However, there has been little data of sufficient quality to help validate the model. The recent fielding of numerous seasonal monitor data by members of the LORIPP has provided useful data for the assessment.

The analysis of the 2006 data presented in this paper shows that the either models (2004 and weather regression) sufficiently bounds the position error over all times. In fact, the data suggests that there is sufficient margin on both models to accept reasonable errors in ASF estimates. In the range domain, the models generally bound the ASF variations though this is not always the case. Some of these instances are explainable due to noise or map granularity which is not account for by the models. Another cause may be common error terms. However, additional analysis is necessary as these models are required to always bound the errors.

6.0 Disclaimer

The views expressed herein are those of the authors and are not to be construed as official or reflecting the views of the U.S. Coast Guard, Federal Aviation Administration, Department of Transportation or Department of Homeland Security or any other person or organization.

7.0 Acknowledgments

The authors gratefully acknowledge the support of the Federal Aviation Administration and Mitchell Narins under Cooperative Agreement 2000-G-028. They are grateful for the support their support of Loran and the activities of the LORIPP.

8.0 Bibliography

[1] FAA report to FAA Vice President for Technical Operations Navigation Services Directorate, “Loran’s Capability to Mitigate the Impact of a GPS Outage on GPS Position, Navigation, and Time Applications,” March 2004.

[2] Robert Wenzel, Peter Morris, and Kirk Montgomery, "An Examination of Loran Signal Propagation Temporal Variation Modeling", Proceedings of the International Loran Association 35th Annual Meeting, Groton, CT, October 2006

[3] J. R. Johler, R. H. Doherty, L. W. Campbell, “Loran-C System Dynamic Model, Temporal Propagation Variation Study,” DOT-CG-D57-79, July 1979

[4] Sherman Lo, et al., "Analysis of ASF for Required Navigation Performance 0.3", Proceedings of the International Loran Association 32nd Annual Meeting, Boulder, CO, November 2003

[5] Sherman Lo, et al., "Loran Availability and Continuity Analysis for Required Navigation Performance 0.3" Proceedings of GNSS 2004 – The European Navigation Conference, Rotterdam, The Netherlands, May 2004